



HAL
open science

Anisotropy of grain boundaries in crystals: a new measurement technique applied to polar ice

Gaël Durand, François Graner, Jérôme Weiss

► **To cite this version:**

Gaël Durand, François Graner, Jérôme Weiss. Anisotropy of grain boundaries in crystals: a new measurement technique applied to polar ice. 2003. hal-00000573v1

HAL Id: hal-00000573

<https://hal.science/hal-00000573v1>

Preprint submitted on 3 Sep 2003 (v1), last revised 22 Jul 2004 (v3)

HAL is a multi-disciplinary open access archive for the deposit and dissemination of scientific research documents, whether they are published or not. The documents may come from teaching and research institutions in France or abroad, or from public or private research centers.

L'archive ouverte pluridisciplinaire **HAL**, est destinée au dépôt et à la diffusion de documents scientifiques de niveau recherche, publiés ou non, émanant des établissements d'enseignement et de recherche français ou étrangers, des laboratoires publics ou privés.

Anisotropy of grain boundaries in crystals: a new measurement technique applied to polar ice

G. DURAND¹, F. GRANER²[*], AND J. WEISS¹

¹ *Laboratoire de Glaciologie et de Géophysique de l'Environnement (FRE 2192 CNRS - Université J. Fourier Grenoble 1), BP 96, F-38402 Saint Martin d'Hères cedex, France*

² *Laboratoire de Spectrométrie Physique (UMR 5588 CNRS - Université J. Fourier Grenoble 1), BP 87, F-38402 Saint Martin d'Hères cedex, France*

PACS. 83.80.Nb – Geological materials: Earth, magma, ice, rocks, etc. .

PACS. 81.70.-q – Nondestructive materials testing and analysis: optical methods.

PACS. 62.20.Fe – Deformation and plasticity (including yield, ductility, and superplasticity).

PACS. 61.72.Mm – Grain and twin boundaries.

Abstract. –

To analyse a polycrystalline material which has undergone mechanical solicitations, we quantify the deformation of grain boundaries. We investigate a pattern which records past deformations: a deep ice core, in Dome Concordia, Antarctica. Its ice microstructure (grain boundaries) is a key feature useful to study ice evolution and to investigate climatic changes. Our method extracts quantitative physical information, such as the anisotropy and the local heterogeneity of the deformation. This leads to a re-examination of current models used in datation. The method also applies to extract quantitative geometrical information from other cellular patterns, ranging from metal processing and biological tissues to foams and granular matter.

Motivations. – A picture contains a large amount of data, from which it is sometimes difficult to extract quantitative, physically relevant information. In this letter, we present a method to characterise a cellular pattern by measuring a geometrical quantity, the “texture tensor” [1], using local spatial averages. We apply this analysis to the grain boundaries (the so-called “microstructure”) of ice samples, and deduce physical properties of the pattern itself: anisotropy, local heterogeneity, distinction between homogeneous regions and shear bands.

We investigate a pattern in which we have access to the record of past deformations: a deep ice core, in Dome Concordia, Antarctica. Polar ice cores are the focus of many investigations because they record the history of climatic changes. The snow accumulates, then transforms into ice, and flows downwards slowly ($\sim 10^{-12} s^{-1}$). A travel down to deep layers of the ice sheet is thus a travel back to several hundred of thousands of years into the past [2].

A crucial step of paleoclimatic studies from ice cores is dating. In Antarctica, counting annual layers is impossible [3]: absolute dating is only possible for the very top of the ice cores where ice layers containing volcanic impurities can be related to historical volcanic eruptions.

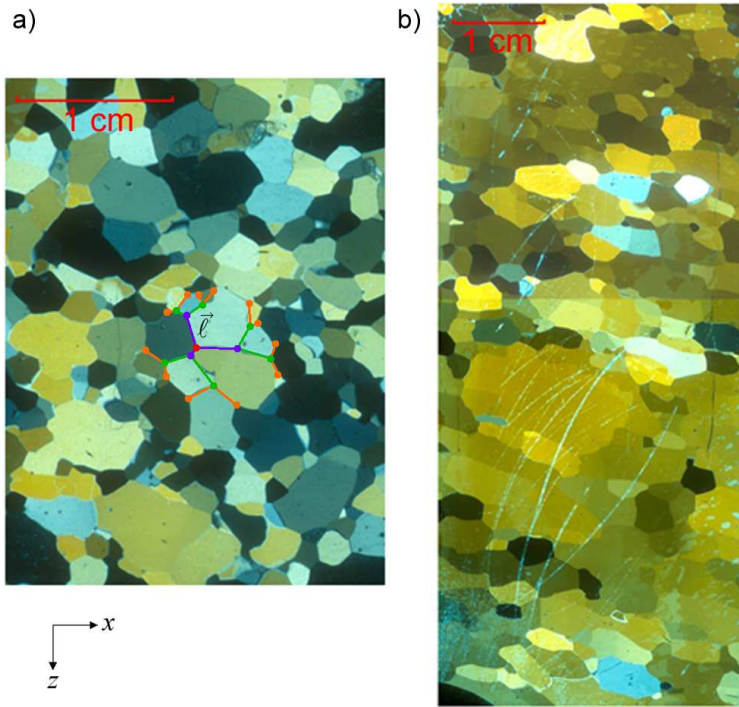


Fig. 1 – Two thin sections of ice imaged between crossed polarisers in white light. Each grain has an almost uniform c -axis orientation, visualised by its color. (a) At 362 m depth, the microstructure looks isotropic; (b) at 2629 m depth the microstructure is visibly anisotropic (the white scratches do not affect the image analysis, which ignores them). Superimposed on (a): notations used in the measurement of \overline{M} . We consider here for instance the site labeled by a red dot. We note $\vec{\ell}$ a vector linking it to one of its neighbours. There are 3 such vectors in the first shell, $p = 1$ (purple); 6 in shell $p = 2$ (green); 12 in shell $p = 3$ (orange).

Below, datation relies on ice sheet flow models of the evolution of ice layer thinning with depth [3]. Such models are loosely constrained by the identification of large climatic transitions for which absolute dating can be obtained on other records (*e.g.* marine sediment cores). For the sake of simplicity, these models assume a smooth and monotonous increase of the thinning with depth, hence ignore any possible localization of the deformation [3, 4].

The results of this letter question this essential assumption, which apparently holds only down to 1200 m in the present case. We first present how the samples are obtained, then the image analysis, and finally the results, which we briefly discuss.

Samples. – Dome Concordia, Antarctica ($75^{\circ} 06' 04''$ S, $123^{\circ} 20' 52''$ E, elevation 3233 m a.s.l.) is at the summit of an Antarctic ice dome, which has been chosen because it is usually assumed that the ice flow is axisymmetric around the vertical (z) axis, and isotropic within the horizontal plane.

The ground is 3309 ± 22 m below the ice surface. An European ice core drilling program (EPICA) reached the depth of 3201.65 m in February 2003. Samples have been extracted and transported according to standard procedures [5]. We analyzed thin (~ 0.1 mm) sections:

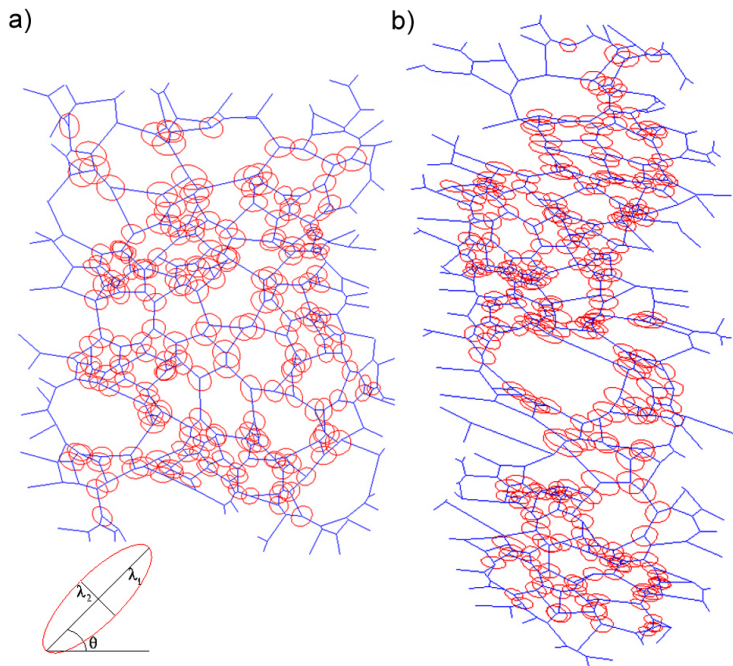


Fig. 2 – Analysis of the images presented in Fig. 1. The texture tensor $\overline{\overline{M}}$ measured at each site is represented as an ellipse, with its axes along the eigenvectors, and its half-axes proportional to eigenvalues λ_1, λ_2 respectively. A site around which the pattern is isotropic is represented by a circle; conversely, a strong anisotropy is represented as an elongated ellipse. The size of the ellipse (same scale for each ellipse) represents the local length of the grain boundaries, i.e quantifies the local grain size. Due to the definition of $\overline{\overline{M}}$ (eq. 1), we exclude sites too close to the image boundary.

each sample is a few cm high, see Fig. (1), with a sampling interval varying from 2 to 50 m. The vertical axis on a thin section always corresponds to the true *in situ* vertical axis z ; its horizontal axis, labelled x in what follows, has an unknown and variable orientation within the true *in situ* horizontal plane.

Image analysis. – The problem we address is to extract physically relevant information from the geometry of this microstructure. While many quantitative descriptors exist [6], few are adapted to the determination of the anisotropy of such a pattern. We chose to use a descriptor introduced in ref. [1]: the local *texture tensor* $\overline{\overline{M}}$, measured as follows.

We have developed [5] a digital image processing of pictures of ice under crossed polarisers, that determines the grain boundaries, then the sites (“vertices”) where three boundaries meet, see Fig. (1). For each given pair of neighbouring sites, we draw the vector which links them and denote it by $\vec{\ell}$ (Fig. 1a).

We construct, for each vector, the tensor $\vec{\ell} \otimes \vec{\ell}$: its coordinates are $(\ell_i \ell_j)$, where i, j are here x or z . This tensor is not sensitive to the sign of the vector (it is invariant under $\vec{\ell} \rightarrow -\vec{\ell}$), but it characterizes its length ℓ and its direction.

To characterize *statistically* the average properties of the pattern, we thus average $\vec{\ell} \otimes \vec{\ell}$. Ref.

[1] originally proposed to take the average over a box of fixed size. Such box should be smaller than the image (in order to visualise local details), but still large enough to include many wall vectors (N should be larger than one, to have relevant statistics). This was convenient for movies [7, 8], where, even if the box was small and did not contain many sites, the average could be taken over many successive images. It resulted in very good statistics [7], even if some links crossed the boundary of the box instead of being fully included in it [8]. Here, we can perform averages over space, not over time. Since grains have variable size (grains grow with time, hence old grains in deep ice are much larger than young grains near the dome surface), it would be difficult to select such a fixed box size.

We thus chose a local averaging, over a few neighbouring sites: $\langle \cdot \rangle$ denotes the average over N vectors, up to the p -th neighbours (Fig. 1a). Hence, at each site we include approximately the same number of vectors, $N \approx 3 + 6 + \dots + 3 \times 2^{p-1}$. We thus measure the local *texture tensor* $\overline{\overline{M}}$ [1] at each given site:

$$\overline{\overline{M}} = \frac{1}{N} \sum_{k=1}^N \vec{\ell}^k \otimes \vec{\ell}^k = \left\langle \left(\begin{array}{cc} \ell_x^2 & \ell_x \ell_z \\ \ell_z \ell_x & \ell_z^2 \end{array} \right) \right\rangle. \quad (1)$$

We find that $p = 3$ (and hence $N = 3 + 6 + 12 = 21$) is a good compromise (Fig. 1a): small enough to visualise local heterogeneities, and large enough to ensure good statistics.

This tensor, independent from crystallographic information, does not require any knowledge or hypothesis regarding the past history of the sample. The diagonal components M_{xx} and M_{zz} of this tensor are both of order of the average square distance between sites, $\langle \ell^2 \rangle$. Conversely, the off-diagonal component $M_{xz} = M_{zx}$ (the tensor is symmetric) is much smaller, and even vanishes when the pattern is isotropic. Hence the tensor $\overline{\overline{M}}$ has two strictly positive eigenvalues $\lambda_1 \geq \lambda_2 > 0$: the largest corresponds to the direction in which grains are most elongated.

Results. – This averaged tensor discards small-scale details and reflects relevant physical features of the actual microstructure of the material, visible in each region of Fig. (2). It first yields qualitative information regarding the deformation and its localisation. The upper sample (at a depth of 362 m) is almost homogeneous: its anisotropy is small, with a horizontal main axis, as could be expected from a sample taken at a dome, undergoing a small vertical compression, with axisymmetry in the xz plane (Fig. 2a). Conversely, the lower sample (depth 2629 m) displays a clear and localised anisotropy, indicating a symmetry breaking (Fig. 2b).

To obtain a more quantitative information, we measure the shape isotropy, which we define for instance as a number comprised between 0 for an extreme anisotropy, represented as an ellipse squashed to a segment, and 1 for a perfect isotropy, represented as a circle:

$$\alpha = \frac{2\lambda_1 \lambda_2}{\lambda_1^2 + \lambda_2^2}. \quad (2)$$

We also denote by θ the angle between the horizontal plane and the eigenvector \vec{e}_1 corresponding to the largest eigenvalue λ_1 ($-90^\circ < \theta \leq 90^\circ$), see Fig. (2).

The upper sample is characterized by isotropies mainly above 0.8; the angle θ is thus widely distributed, although concentrated around 0° , in agreement with a vertical compression (Fig. 3a). Conversely, the lower sample is more anisotropic: its isotropies are distributed between 0.2 and 1, and it has a marked preferred orientation $\theta \approx 20^\circ$ (Fig. 3b).

Equipped with such tools, we can now turn to a systematic investigation of all available ice thin sections, that is, quantify the dependence of patterns with the depth. For each image, we measure $\overline{\overline{M}}$ from eq. (1) by averaging over all the vectors (*i.e.* all grain boundaries) of

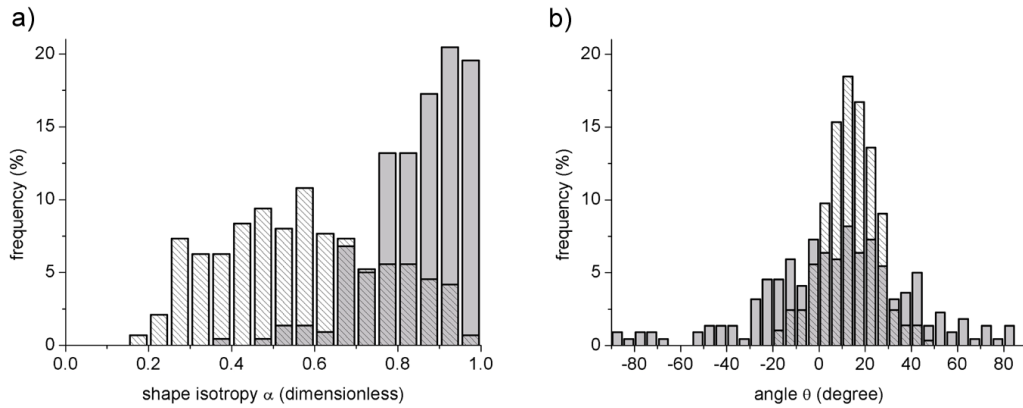


Fig. 3 – Histogram of shape isotropy α and orientation θ of the texture tensors measured on Fig. (2a): 362 m deep sample (grey) and on Fig. (2b): 2629 m deep sample (hatched).

the sample. We then calculate the global isotropy of the sample from eq. (2). We observe a small heterogeneity of samples, until around 1200 m; below that depth, the isotropy saturates around 0.9, while the heterogeneity strikingly increases.

To check the significance of these fluctuations, we measure the isotropy using a sliding window over a half meter long section (at $z = 335$ m, corresponding to the Holocene period, a climatically quiet zone). We check that the distribution of isotropies is roughly gaussian (data not shown), and measure its standard deviation σ . This defines $\pm 2\sigma = 95\%$ and $\pm 3\sigma = 99.7\%$ confidence intervals, appearing on Fig. (4a). Data points exceed this interval,

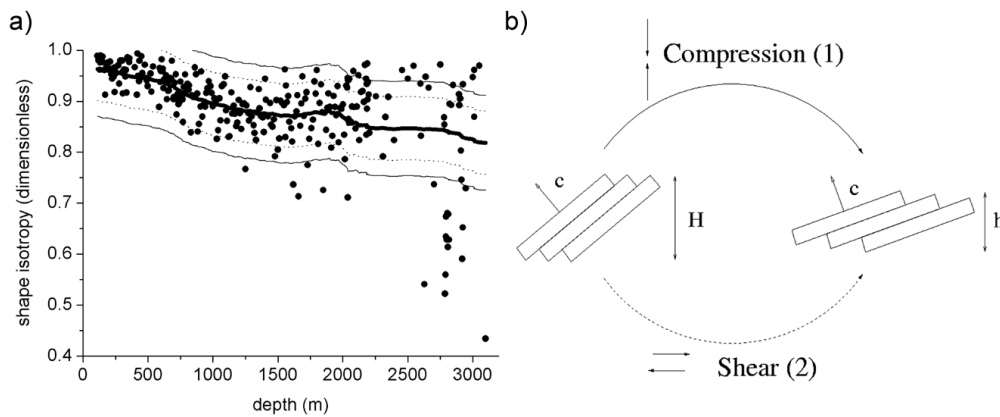


Fig. 4 – (a) The shape isotropy of the ice microstructure, plotted *versus* the depth inside the ice core. Each point corresponds to one of 303 samples; each sample (except for nine of them) comprises at least 100 sites, and up to 1000 sites for the upper samples. Thick solid line: average, defined by a sliding window over 100 points; dashed lines and thin solid lines: 95% and 99.7% confidence intervals (see text). (b) Scheme representing the deformation mechanisms acting near a dome. Both vertical compression (1) and horizontal shear (2) induce a rotation of the c axes of the grains towards the vertical z axis; hence ice grains of height H become thinner ($h < H$).

denoting anomalously small or large isotropies.

Strikingly, the isotropy undergoes a strong heterogeneity, over a scale as small as the distance between consecutive samples (down to 2 m). The deformation exhibits localization that increases with depth, with deformed layers beside non-deformed ones.

Discussion. – In the light of these results, let us now re-examine how datation charts are established, that is, the relation $t(z)$ between depth z and age t of ice. Datation is based on the thinning ε_{zz} of the ice, defined as the ratio:

$$\varepsilon_{zz} = e_{zz}/e_{zz}(z = 0),$$

where e_{zz} is the thickness of the ice layer at depth z . As mentioned in the introduction, to transpose depth into ice age requires a model for the evolution of the deformation rate $\partial\varepsilon_{zz}/\partial z$ with depth. Current models assume smooth and positive profile of $\partial\varepsilon_{zz}/\partial z$, therefore a smooth and monotonous increase of the thinning.

At a dome, axisymmetry implies in principle that thinning of the ice results from vertical compression only. The ice core drilled exactly at the summit of a dome is thus easier to model assuming the flow is axisymmetric. The main drawbacks of such simplified models are already well-known. Let us summarise them briefly.

First, due to the horizontal component of the ice flow, the contribution of shear to thinning becomes predominant already at a few kilometers beside the dome [9]. Noteworthy, in practice, even below the dome, the flow is never purely vertical, as the result of an irregular bed rock topography [9] and of a possible motion of the dome location with time [10]. Consequently, one can expect a significant role of horizontal shear in the lower part [11].

Second, ice grains are hexagonal crystals, and their viscoplastic deformation is very anisotropic, as slip occurs mainly along the basal planes [12]. Consequently, vertical compression or horizontal shear induce a rotation of the c axes of the grains towards the vertical z axis [11, 13]. Hence, even when the axisymmetry is observed at large scale, it is usually broken at the grain scale (Fig. 4b).

Here, we observe a striking heterogeneity, that is, difference between the isotropy of two samples close to each other. We can suggest a possible explanation. As mentioned above, under shear deformation (Fig. 4b (1)), the c axis of a grain rotates towards the vertical z axis (“formation of fabric”) [13]. In turn, such grain becomes more sensitive to horizontal shear. This creates a positive feedback, and can induce a bifurcation process: small differences in shear deformation (and therefore in thinning) between adjacent layers are constantly reinforced [11]. On the opposite, deformed grains become less sensitive to vertical compression [11] (Fig. 4b (2)): in the regions where vertical compression dominates, the feedback should be negative, hence less heterogeneities. This explanation is compatible with our observation of a strong heterogeneity only in the regions deeper than 1200 m, where shear dominates (Fig. 4b). Such positive feedback could lead to arbitrarily high local differences in flow rates, which is in contradiction with the hypothesis of the datation model.

This could require a revision of the current standard datation charts, especially at frequencies higher than those associated with large climatic variations (glacial-interglacial fluctuations). Unfortunately, besides grain deformation, other processes (normal grain growth, recrystallization) modify the ice microstructure through depth and time. For that reason, the microstructure does not record completely the thinning ε_{zz} . Hence ε_{zz} is not directly measurable, and the isotropy α underestimates it. This precludes a direct use of the present results to date the ice by integration of ε_{zz} from the top.

Perspectives. – In the future, we expect to correlate the grain boundary pattern with the c -axis orientations, to go further into our understanding of their coupling. We are also cur-

rently applying our measurement of the grain isotropy to correct and improve the estimation of their 3D volume from 2D cuts.

Our method is based on a local average over space, not over time. Since it is based on boxes of constant “topological” (constant number of shells) rather than “geometrical” (usual) size, the number N of links in the average, and hence the statistics, have the same meaning throughout even a heterogeneous sample. It applies to similar cellular patterns in very different systems, including foams [14]. We currently plan to analyze biological tissues [15] or granular matter [16], and even fracture patterns. Other possibilities include the characterization of microstructure in various polycrystalline materials, such as metals during industrial processes, or geological rocks in tectonical flows.

* * *

We thank M. Aubouy for his support and useful discussions. This work was partially supported by CNRS ATIP 0693. This work is a contribution to the “European project for Ice Coring in Antarctica” (EPICA), a joint ESF (European Science Foundation)/EC scientific program, funded by the European Commission under the Environment and Climate Programme (1994-1998) contract ANV4-CT95-0074 and by national contributions from Belgium, Denmark, France, Germany, Italy, the Netherlands, Norway, Sweden, Switzerland and the United Kingdom.

REFERENCES

- [*] Author for correspondence at graner@ujf-grenoble.fr. Fax: (+33) 4 76 51 45 44.
- [1] AUBOUY M., JIANG Y., GLAZIER J. A. and GRANER F., *Granular Matt.*, **5** (2003) 67.
- [2] PETIT J.R., JOUZEL J., RAYNAUD D., BARKOV N.I., BARNOLA J.M., BASILE I., BENDER M., CHAPPELLAZ J., DAVIS M., DELAYGUE G., DELMOTTE M., KOTLYAKOV V.M., LEGAND M., LIPENKOV V.Y., LORIUS C., PEPIN L., RITZ C., SALTZMAN E. and STIEVENARD M., *Nature*, **399** (1999) 429.
- [3] SCHWANDER J., JOUZEL J., HAMMER C.U., PETIT J.R., UDISTI R. AND WOLFF E. , *Geophysical research letters*, **28** (2001) 4243.
- [4] HAMMER C.U., CLAUSEN H.B., DANSGAARD W., GUNDESTRUP N., JOHNSEN S.J. and REEH N., *J. Glacio.*, **20** (1978) 3.
- [5] GAY M., and WEISS J., *J. Glaciol.*, **45** (1999) 547.
- [6] MECKE K. and STOYAN D. (Editors), *Morphology of Condensed Matter - Physics and Geometry of Spatially Complex Systems, Lecture Notes in Physics*, Vol. **600** (Springer, Heidelberg) 2002
- [7] ASIPAUSKAS M., AUBOUY M., GLAZIER J. A., GRANER F. and JIANG Y., *Granular Matt.*, **5** (2003) 71.
- [8] JANIAUD E. and GRANER F., preprint (2003), cond-mat/0306590
- [9] MANGENAY A., CALIFANO F. and HUTTER K., *J. Geophys. Res.*, **102** (1997) 22749.
- [10] ANANDAKRISHNAN S. and ALLEY R.B., *Geophysical research letters*, **21** (1994) 441.
- [11] ALLEY R.B., GOW A.J., MEESE D.A., FITZPATRICK J.J., WASHINGTON E.D. and BOLZAM J.F., *J. Geophys. Res.*, **102** (1997) 26819.
- [12] DUVAL P., ASHBY M.F. and ANDERMAN I., *J. Phys. Chem.*, **87** (1983) 4066.
- [13] ALLEY R.B., *Science*, **240** (1988) 493.
- [14] COURTY S., DOLLET B., ELIAS F., HEINIG P. and GRANER F., preprint (2003), cond-mat/0305408.
- [15] LECUIT, T., preprint.
- [16] KOLB E. and CLAUDIN P., private communication.